# $MoF_6$ and $WF_6$: Nonrigid Molecules?

**Gustavo Santiso Quiñones,[a] Gerhard Hägele,[b] and Konrad Seppelt*[a]**

**Abstract:** Calculations reveal that the octahedral–trigonal prismatic–octahedral rearrangement has particularly low-energy barriers for $MoF_6$, $WF_6$, and (hypothetical) $CrF_6$. Experimental evidence is obtained from the dynamic $^{19}F$ NMR spectra of the derivatives $CF_3–CH_2–O–MoF_5$, $CF_3–CH_2–O–WF_5$, $C_6F_5–O–MoF_5$, $C_6F_5–O–WF_5$, and $(CF_3)_3C–O–WF_5$. The ground-state structure of all these compounds is octahedral; at elevated temperatures the nonequivalent metal-bound fluorine atoms undergo an intramolecular exchange. The exchange mechanism could be a 3+3 or a 2+4 twist; calculations favor the 3+3 twist.

**Keywords:** $^{19}F$ NMR spectroscopy · fluorides · fluxionality · molybdenum · nonrigid structures · tungsten

## Introduction

The octahedron represents the principal structure for the vast majority of six-coordinate complex molecules. Recently this paradigm has been questioned, since stoichiometrically simple compounds like $Mo(CH_3)_6$, $W(CH_3)_6$, or $Re(CH_3)_6$ are distorted or regular trigonal prismatic.[1] There exist a fairly large number of binary hexafluorides, including main group (S, Se, Te, Xe), transition-metal (Mo, Tc, Ru, Rh, W, Re, Os, Ir, Pt), and actinide elements (U, Np, Pa), that are all octahedral (with the single but now well-understood exception of $XeF_6$); although $Mo(CH_3)_6$ and $MoF_6$, $W(CH_3)_6$, and $WF_6$, $Re(CH_3)_6$ and $ReF_6$ are isoelectronic. If one accepts the distorted trigonal prismatic structure, for example, for the 12-electron $Mo(CH_3)_6$ system as ground state, as theory demands, then the octahedral structure of, for example, $MoF_6$ can be explained by one or both of the following effects: 1) The fairly high partial negative charge on the fluorine ligands results in a strong repulsion effect, which favors the octahedron as the geometry with the least ligand repulsion of all possible six-coordinate structures. 2) In contrast to $Mo(CH_3)_6$, there exists in $MoF_6$ a considerable ligand-to-central-atom electron back donation. This raises the electron count on molybdenum above 12, and at the latest at 18-valence electrons the octahedron will prevail.

While there is no doubt that $MoF_6$ and $WF_6$ are octahedral, also for derivatives such as $W(OCH_3)_6$[2,3] or $W(NR_2)_6$,[4] which carry nonbonding electron pairs on the ligands, the question raised here is how close in energy a trigonal-prismatic structure would be. If it is close to 10 kcal mol$^{-1}$, then it can be assumed that the molecules would show fluxionality at ambient or slightly elevated temperatures, so that they could be called nonrigid. This is difficult to prove by experiment, since all fluorine atoms in $MoF_6$ and $WF_6$ remain equal before and after the rearrangement. We therefore decided to answer this question by a typical chemical approach, namely by replacing one fluorine atom with a ligand that displays similar chemical behavior. The auxiliary ligands $CF_3–CH_2–O–$, $C_6F_5–O–$, and $(CF_3)_3C–O–$ have been chosen because they are fairly easy to introduce, and the resulting compounds are at least in part stable enough for subsequent high-temperature NMR investigations.

## Results

**Theoretical predictions for $MoF_6$, $WF_6$, $CF_3–CH_2–O–MoF_5$, $CF_3–CH_2–O–WF_5$, $C_6F_5–O–MoF_5$, $C_6F_5–O–WF_5$, $(CF_3)_3C–O–MoF_5$, and $(CF_3)_3C–O–WF_5$**: All calculations were done on the density functional level of theory, Becke 3 LYP method. For details see the Experimental Section. The octahedral–trigonal-prismatic rearrangement barrier has been calculated before,[1] for present calculations see Table 1. As expected, the ground state for $MoF_6$ and $WF_6$, as well for $CrF_6$, $NbF_6^-$, $TcF_6^+$, and $ReF_6^+$, is octahedral. The calculated M–F bond lengths are about 4 pm longer

[a] M. Sc. G. Santiso Quiñones, Prof. Dr. K. Seppelt
Freie Universität Berlin
Institut für Chemie, Anorganische und Analytische Chemie
Fabeckstrasse 34–36, 14195 Berlin (Germany)
Fax: (+030) 838-53310
E-mail: seppelt@chemie.fu-berlin.de

[b] Prof. Dr. G. Hägele
Institut für Anorg. Chemie und Strukturchemie I
Universität Düsseldorf
Universitätsstrasse 1, 40225 Düsseldorf (Germany)
Fax (+49) 221-8113085
E-mail: haegele@uni-duesseldorf.de

 **DOI: 10.1002/chem.200400095**  

Table 1. DFT calculations on selected molecular, anionic, and cationic hexafluorides: energies, bond lengths, and lowest vibrational frequency.

| | | Energy + zero point energy [a.u.] | $r_{M-F}$ [pm] | $\nu$ [$cm^{-1}$][a] | $\Delta E$ [kcal $mol^{-1}$] |
|---|---|---|---|---|---|
| $CrF_6$ | $O_h$ | −686.172442 | 174.0 | 129.9 | 0.0 |
| | $D_{3h}$ | −686.152051 | 174.8 | 97.5i | 12.7 |
| $MoF_6$ | $O_h$ | −667.592595 | 186.6(182.0(3)[b]) | 91.2 (116)[c] | 0.0 |
| | $D_{3h}$ | −667.582059 | 186.9 | 49.0i | 6.6 |
| $WF_6$ | $O_h$ | −666.564772 | 187.5 (183.2(3)[d]) | 111.5 (127)[c] | 0.0 |
| | $D_{3h}$ | −666.547373 | 188.0 | 75.5i | 10.9 |
| $NbF_6^-$ | $O_h$ | −656.667833 | 193.9 | 99.3 | 0.0 |
| | $D_{3h}$ | −656.651896 | 194.2 | 74.5i | 10.0 |
| $TcF_6^+$ | $O_h$ | −679.601872 | 182.6 | 76.5 | 0.0 |
| | $D_{3h}$ | −679.594678 | 183.1 | 39.0i | 4.4 |
| $ReF_6^+$ | $O_h$ | −677.203127 | 183.4 | 109.1 | 0.0 |
| | $D_{3h}$ | −677.188196 | 184.1 | 72.0i | 9.4 |

[a] Lowest calculated vibrational frequencies, $T_{2u}$ in $O_h$, imaginary frequencies $A_1''$ in $D_{3h}$. [b] Experimental value, see ref [5]. [c] Experimental value, see ref [6,7]. [d] Experimental value, see ref. [5,8].

than those for which experimental values are known. In all cases, the trigonal-prismatic structure is a transition state, as is evidenced by one imaginary frequency. The M–F bond lengths in the transition state are marginally longer than in the octahedral ground state, reflecting the small loss of energy. It is evident that in $MoF_6$ this $O_h$–$D_{3h}$ barrier is even lower than in $CrF_6$ and $WF_6$. That the barrier in $MoF_6$ is lower than that in $CrF_6$ can be explained by the increased size of the $MoF_6$ molecule, which results in lower interligand repulsion, making the trigonal-prismatic structure more favorable. The higher barrier in $WF_6$ is explained by the influence of the strongly increased relativistic effect: The W–F bond lengths are only slightly longer than the Mo–F bond lengths, but the polarity of the bond is increased.

In the series $NbF_6^-$, $MoF_6$, and $TcF_6^+$, the decreasing bond polarity favors the trigonal-prismatic structure, so that for the unknown $TcF_6^+$ ion the octahedral structure is no longer guaranteed if the errors of the DFT calculations are taken somewhat generously.

Looking at all known hexafluorides (except $XeF_6$) clearly reveals the exceptional case of $MoF_6$. The $\nu_6$ ($T_{2u}$) vibration (both IR and Raman forbidden) of these octahedral molecules has the lowest value for $MoF_6$ (Table 2). This is because this vibration contributes to the octahedral–trigonal-prismatic rearrangement (see Figure 1; for simplification the structures of the $d^1$-$d^4$ hexafluorides $ReF_6$–$PtF_6$, and $TcF_6$–$RhF_6$ are considered to be octahedral, although some of them may exhibit very small Jahn–Teller distortions[9–11]).

The exact mechanism of the ligand exchange in $MoF_6$ is difficult to prove, in contrast to that in five-coordinate species like $PF_5$, for which a 2+2 exchange mechanism (Berry pseudorotation) can be differentiated from a 3+2 exchange mechanism (Turnstile rotation). In $MoF_6$, the aesthetically more pleasing exchange mechanism would be of a 3+3 type (see Figure 1a), which is sometimes called a Bailar twist, named after J. C Bailar, Jr. who first mentioned it in the literature in 1958.[12] Here the reaction coordinate is the twist angle between the two sets of triangular positioned ligands with $\alpha = 60°$ for the octahedron and $\alpha = 0°$ for the trigonal prism. Interestingly, a 2+4 ligand twist (with $\beta = 0°$ for the octahedron, see Figure 1b) would result also in a regular trigonal prism with $\beta = 45°$.[13] Simulated dynamic $^{19}F$ NMR spectra for R–O–$MF_5$ molecules show no difference between these two mechanisms, so they are experimentally undistinguishable. The argument favoring the 3+3 mechanism (Figure 1a) is derived by calculation: All calculated trigonal-prismatic structures have one imaginary frequency for all the compounds discussed here, and the vector of this vibration is identical to the reaction coordinate of the 3+3 mechanism.

The DFT calculations of the monosubstituted derivatives R–O–$MoF_5$ and R–O–$WF_5$ are summarized in Table 3. Again the major difference is that experimental Mo–F bond lengths (see below) are a few pm shorter than calculated. The energy difference between the octahedral ground state

Table 2. Experimental values [$cm^{-1}$] for the Raman- and IR-forbidden $\nu_6$ ($T_{2u}$) vibration of molecular octahedral hexafluorides.[6]

| | | | | | |
|---|---|---|---|---|---|
| | | | | | $SF_6$ |
| | | | | | 347 |
| | | | | | $SeF_6$ |
| | | | | | 264 |
| $MoF_6$ | $TcF_6$ | $RuF_6$ | $RhF_6$ | | $TeF_6$ |
| 116 | 145 | 186 | 192 | | 197 |
| $WF_6$ | $ReF_6$ | $OsF_6$ | $IrF_6$ | $PtF_6$ | |
| 127 | 193 | 205 | 206 | 211 | |
| $UF_6$ | $NpF_6$ | $PuF_6$ | | | |
| 142 | 164 | 173 | | | |

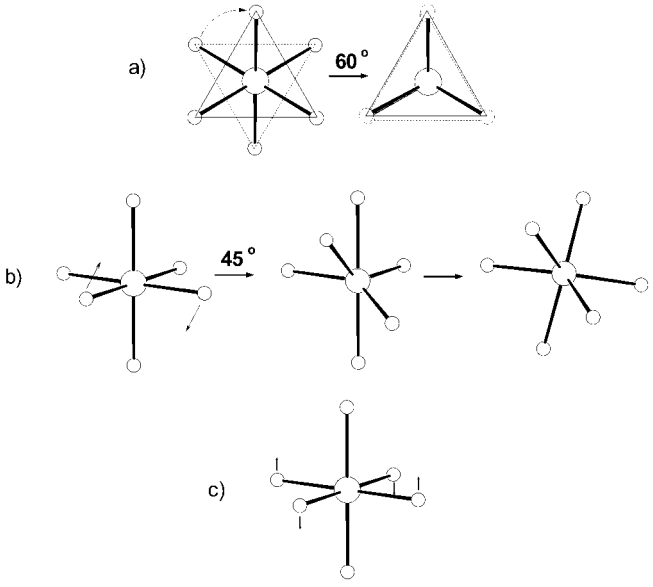


Figure 1. a) The 3+3 octahedral–trigonal-prismatic rearrangement reaction coordinate is the twist angle between the two trigonal sets of ligands. b) The 2+4 octahedral–trigonal-prismatic rearrangement. The reaction coordinate is the twist angle between two *cis*-oriented ligands relative to the other four. c) The Raman- and IR-forbidden $\nu_6(T_{2u})$ vibration of the octahedron, which is a component of both the 3+3 and 4+2 rearrangements.

Table 3. Results of DFT calculations on $CF_3$–$CH_2$–O–$MF_5$, $C_6F_5$–O–$MF_5$, $(CF_3)_3C$–O–$MF_5$; M = Mo, W.

| | Energy + zero point energy [a.u] | $\Delta E$ [kcal mol$^{-1}$] | Bond lengths [pm] | |
|---|---|---|---|---|
| $CF_3$–$CH_2$–O–$MoF_5$ ($O_h$) | −1019.983954 | 0 | Mo–O | 185.2 |
| | | | Mo–$F_{ax}$ | 187.2 |
| | | | Mo–$F_{eq}$ | 187.2–190.2 |
| | | | C–O | 140.3 |
| $CF_3$–$CH_2$–O–$MoF_5$ ($D_{3h}$) | −1019.967650 | 10.23 | Mo–O | 188.2 |
| | | | Mo–$F_{1,2,3}$ | 187.0–187.8 |
| | | | Mo–$F_{4,5}$ | 189.2 |
| | | | C–O | 141.6 |
| $CF_3$–$CH_2$–O–$WF_5$ ($O_h$) | −1018.951387 | 0 | W–0 | 186.0 |
| | | | W–$F_{ax}$ | 188.4 |
| | | | W–$F_{eq}$ | 188.1–190.3 |
| | | | C–O | 140.5 |
| $CF_3$–$CH_2$–O–$WF_5$ ($D_{3h}$) | −1018.928884 | 14.12 | W–O | 188.8 |
| | | | W–$F_{1,2,3}$ | 188.1–188.8 |
| | | | W–$F_{4,5}$ | 190.1 |
| | | | C–O | 141.9 |
| $C_6F_5$–O–$MoF_5$ ($O_h$) | −1370.901500 | 0 | Mo–O | 188.4 |
| | | | Mo–$F_{ax}$ | 186.8 |
| | | | Mo–$F_{eq}$ | 187.4–189.9 |
| | | | C–O | 132.3 |
| $C_6F_5$–O–$MoF_5$ ($D_{3h}$) | −1370.88428 | 10.81 | Mo–O | 193.6 |
| | | | Mo–$F_{1,2,3}$ | 186.6–187.6 |
| | | | Mo–$F_{4,5}$ | 189.0–189.1 |
| | | | C–O | 133.4 |
| $C_6F_5$–O–$WF_5$ ($O_h$) | −1369.867201 | 0 | W–O | 187.4 |
| | | | W–$F_{ax}$ | 187.9 |
| | | | W–$F_{eq}$ | 188.4–189.2 |
| | | | C–O | 133.2 |
| $C_6F_5$–O–$WF_5$ ($D_{3h}$) | −1369.842479 | 15.51 | W–O | 191.8 |
| | | | W–$F_{1,2,3}$ | 188.0–188.6 |
| | | | W–$F_{4,5}$ | 189.5 |
| | | | C–O | 135.0 |
| $(CF_3)_3C$–O–$MoF_5$ ($O_h$) | −1694.214825 | 0 | Mo–O | 186.5 |
| | | | Mo–$F_{ax}$ | 186.6 |
| | | | Mo–$F_{eq}$ | 187.4–187.7 |
| | | | C–O | 137.9 |
| $(CF_3)_3C$–O–$MoF_5$ ($D_{3h}$) | −1694.194078 | 13.02 | Mo–O | 186.5 |
| | | | Mo–$F_{1,2,3}$ | 187.4–187.7 |
| | | | Mo–$F_{4,5}$ | 187.5, 186.6 |
| | | | C–O | 137.9 |
| $(CF_3)_3C$–O–$WF_5$ ($O_h$) | −1693.184774 | 0 | W–O | 187.2 |
| | | | W–$F_{ax}$ | 187.6 |
| | | | W–$F_{eq}$ | 188.3–188.4 |
| | | | C–O | 138.1 |
| $(CF_3)_3C$–O–$WF_5$ ($D_{3h}$) | −1693.158812 | 16.29 | W–O | 188.7 |
| | | | W–$F_{1,2,3}$ | 188.3–189.7 |
| | | | W–$F_{4,5}$ | 188.7, 188.8 |
| | | | C–O | 138.4 |

and the trigonal-prismatic excited state is calculated to be around 10 kcal mol$^{-1}$ for the three molybdenum compounds and around 15 kcal mol$^{-1}$ for the three tungsten compounds.

**Preparation of $CF_3$–$CH_2$–O–$MoF_5$, $CF_3$–$CH_2$–O–$WF_5$, $C_6F_5$–O–$MoF_5$, $C_6F_5$–O–$WF_5$, and $(CF_3)_3C$–O–$WF_5$, structural determinations**: These monosubstituted derivatives of $MoF_6$ and $WF_6$ are readily prepared by variations of literature procedures [Eq. (1) and (2)].

$$MF_6 + R{-}O{-}Si(CH_3)_3 \rightarrow R{-}O{-}MF_5 + (CH_3)_3SiF \quad (1)$$
$$M = Mo, W;\ R = CF_3{-}CH_2{-}, C_6F_5{-}$$

$$WF_6 + LiOC(CF_3)_3 \rightarrow (CF_3)_3C{-}O{-}WF_5 + LiF \quad (2)$$

$LiO(CF_3)_3$ gave just the tungsten derivative, it does not react with $MoF_6$. Under suitable conditions only single substitution is observed. Four of these compounds are liquids at room temperature, and $C_6F_5$–O–$MoF_5$ is a solid. All these compounds are characterized by NMR and vibrational spectra and elemental analyses; a single-crystal structure determination was carried out for $C_6F_5$–O–$MoF_5$. The structure around the metal center in all five compounds is octahedral, as is evidenced by the $AB_4$ patterns in the $^{19}F$ NMR spectra at room temperature or below. Further proof comes from the single-crystal structure determination of $C_6F_5$–O–$MoF_5$, which delivers structural details (Table 4 and Figure 2). It may be of interest that $C_6F_5$–O–$MoF_5$ is deeply colored in the condensed phase. In the crystal structure, there is an intermolecular interaction between the $C_6F_5$ ring of one molecule and the $MoF_5$ group of another molecule, which results in a charge-transfer interaction in which the aromatic ring is clearly the donor and the O–$MoF_5$ group the acceptor. Aside from this finding, the structure is completely as expected. Reaction between $MoF_6$ and $CF_3$–$CH_2$–O–$Si(CH_3)_3$ does not produce solely $CF_3$–$CH_2$–O–$MoF_5$. At longer reaction times and especially if $CF_3$–$CH_2$–O–$Si(CH_3)_3$ is applied in excess, *cis*-$[(CF_3CH_2O)_2MoF_4]$ is detectable as a by-product. This is indicated by the $A_2B_2$ spectrum of the molybdenum-bound fluorine atoms. This compound crystallizes spontaneously from the reaction mixture, and geometrical data from the single-crystal structure determination are collected in Table 4. The *cis* orientation of the two $CF_3$–$CH_2$–O groups within the octahedral molybdenum environment is confirmed.

**Dynamic $^{19}F$ NMR spectra of $CF_3$–$CH_2$–O–$MoF_5$, $CF_3$–$CH_2$–O–$WF_5$, $C_6F_5$–O–$MoF_5$, $C_6F_5$–O–$WF_5$, and $(CF_3)_3C$–O–$WF_5$**: All five compounds under investigation exhibit strongly temperature-dependent $^{19}F$ NMR spectra for the metal-bound fluorine atoms, while the typical $^{19}F$ NMR (and $^1H$ NMR) spectra of the $CF_3CH_2O$–, $C_6F_5O$–, and $(CF_3)_3$-

  

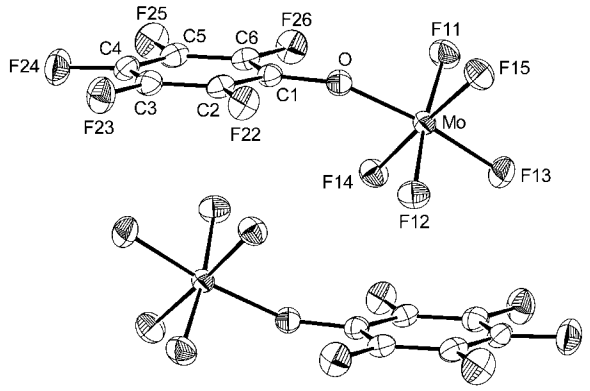


Figure 2. Crystal structure of $C_6F_5$–O–$MoF_5$ (50% probability plot). Shown is a pair of molecules that have a mutual charge-transfer interaction that results in a deep color. The second molecule is generated by the inversion center.

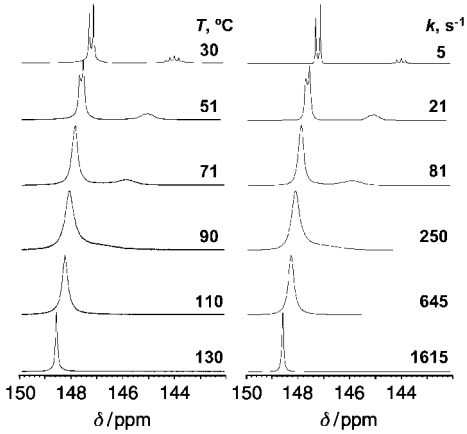


Figure 3. Experimental (left) and simulated (right) temperature-dependent $^{19}F$ NMR (376 MHz) spectra of $C_6F_5$–O–$WF_5$.

Table 4. Experimental bond lengths [pm] and selected bond angles [°] of $C_6F_5$–O–$MoF_5$ and *cis*-[$(CF_3CH_2O)_2MoF_4$].

| | $C_6F_5$–O–$MoF_5$ | | *cis*-[$(CF_3CH_2O)_2MoF_4$] |
|---|---|---|---|
| Mo–O | 182.7(2) | | 178.5(4)–179.2(4) |
| Mo–$F_{ax}$ | 184.4(2) | | |
| Mo–$F_{eq}$ | 182.7(2)–184.7(2) | Mo–F | 184.0(4)–185.3(4) |
| C–O | 133.0(3) | | 140.5(6)–142.1(6) |
| C–C | 137.1(4)–139.8(4) | | 147.8(9)–150.9(9) |
| C–F | 132.1(3)–133.0(3) | | 126.2(9)–133.5(8) |
| $F_{ax}$–Mo–O | 170.8(1) | O–Mo–O | 98.2(2), 98.3(2) |
| $F_{eq}$–Mo–O | 85.8(1)–97.1(1) | F–Mo–F | 83.8(2)–89.1(2), 171.8(2), 171.7(2) |
| Mo–O–C | 149.8(2) | | 144.1(4), 144.7(4) |

C–O– groups are less sensitive towards temperature and hence insignificant for this study. The numerical data for these groups are given in the Experimental Section and will not be discussed any further.

The typical $AB_4$ spectra (approximately doublet + quintet) of the –$OMF_5$ groups are best resolved at room temperature or below. Upon warming, line broadening takes place. The A and $B_4$ parts exhibit intrinsic shifts upfield with increasing temperature, and the apical fluorine is more sensitive than the four equatorial fluorine atoms. Consequently, the second-order character of the underlying $AB_4$ spectrum increases since $\Delta_\delta = \delta_{B4} - \delta_A$ decreases with increasing temperature. At higher temperatures coalescence is observed and further heating results in a sharpening of the remaining single line (Figure 3). The high-temperature limit of the spectra could only be obtained in the case of $C_6F_5$–O–$WF_5$, since our spectrometers have an upper temperature limit of 185 °C for the 90 MHz and 150 °C for the 400 MHz instrument. The molybdenum compounds start to decompose at these temperatures.

It is clear that fluorine exchange of the metal-bound fluorine atoms is occurring. Is this exchange intra- or intermolecular? In the case of $C_6F_5$–O–$WF_5$ we can give definite proof that the exchange is intramolecular. The tungsten-bound fluorine atoms have side bands from $^{183}W$ ($I = 1/2$, 14% natural abundance). These side bands are still visible at the high temperature limit (Figure 4), which shows that the five fluorine atoms remain bound to the tungsten atom. For the molybdenum atoms this method is not available, since the satellites from the only NMR-active isotopes of Mo ($^{95/97}Mo$, $I = 5/2$, 15.9, 9.6% natural abundance) are not observed except in highly symmetric molecules such as $MoF_6$. In the case of $C_6F_5$–O–$MoF_5$, temperature-dependent $^{19}F$ NMR spectra at different concentrations in different solvents ($C_2D_2Cl_4$ and $CD_2Cl_2$) did not show concentration dependence. There is yet another argument against intermolecular exchange: If one assumes that upon heating the metal-bound fluorine atoms could move from one metal atom to another, the OR groups could as well. This would result in a scrambling of F and OR groups and therefore in the formation of some or all members of $(RO)_nMF_{6-n}$ compounds. This is indeed ob-

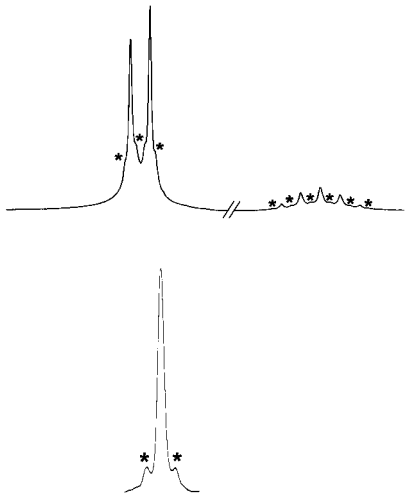

Figure 4. The low- (30 °C) and high-temperature (184 °C) limit $^{19}F$ NMR (84.25 MHz) spectra of $C_6F_5$–O–$WF_5$ at high resolution, showing the $^{183}W$–$^{19}F$ satellite lines, marked by *, arbitrary scales.

served, but only at temperatures above 100 °C and at a very slow rate, so that no coalescence of this type is seen.

The $^{19}$F NMR spectra were successfully simulated (see Figure 3) by using the program *g*NMR. Spin enumeration and permutational operators used for *g*NMR, assuming the aforementioned 3+3 or 2+4 torsional mechanisms, are defined in Figure 5.

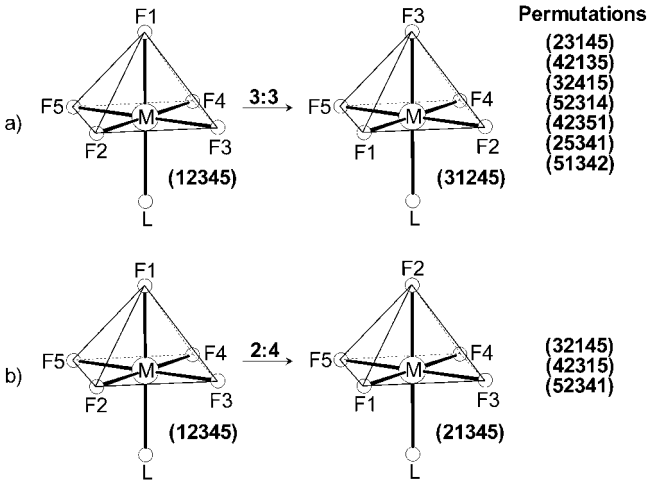


Figure 5. Definition of permutation operators used to describe the 3+3 (a) and 2+4 (b) exchange for compounds of the type $F_5M{-}OR$ (R = $-CH_2{-}CF_3$, $-C_6F_5$, for M = Mo, W; R = $-C(CF_3)_3$ for M = W).

A series of meticulous simulations yielded rate constants for specific temperatures (Table 5). Using the standard linearized Eyring equation $\ln(\frac{k}{T}) = \frac{\Delta H^*}{RT} + \ln(\frac{kk_B}{h} + \frac{\Delta S^*}{R})$, activation energies were estimated as shown in Figure 6. Clearly an agreeable linear behavior is achieved by experiment. The following data were found: $CF_3{-}CH_2{-}O{-}MoF_5$ 12.6, $C_6F_5{-}O{-}MoF_5$ 12.3, $CF_3{-}CH_2{-}O{-}WF_5$ 13.0, $C_6F_5{-}O{-}WF_5$ 13.4, and $(CF_3)_3C{-}O{-}WF_5$ 15.9 kcal mol$^{-1}$, which correspond to $\Delta H^*$ for the octahedral–trigonal-prismatic interchange described above as the 3+3 mechanism. These values can be compared with calculated energies (Table 3). Calculated and experimental energy barriers agree fairly well. We must keep in mind that simulations of these dynamic $^{19}$F NMR spectra are not trivial, mainly because there is a strong temperature dependence of both chemical shifts, especially of the apical fluorine atom, and because of the high second-order character of the $AB_4$ systems. The errors of the experimentally determined activation energies can only be guessed. Slight variation of some of the parameters change the energy values by about 0.5 kcal mol$^{-1}$.

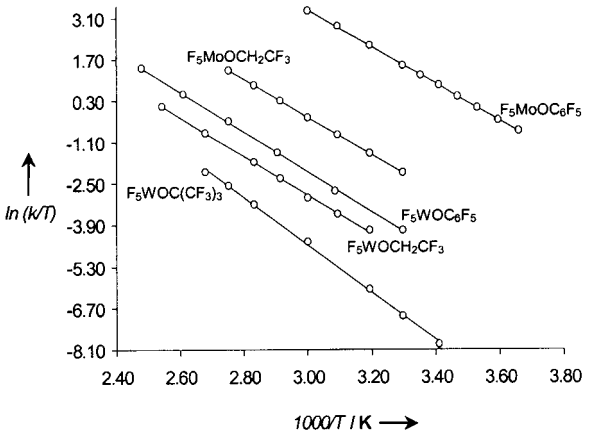


Figure 6. Eyring plot $\ln(\frac{k}{T})$ versus $\frac{1000}{T}$ for rate constants obtained by NMR simulation.

## Conclusion and Outlook

Octahedral $MoF_6$, $WF_6$, and their derivatives $R{-}O{-}MoF_5$ and $R{-}O{-}WF_5$ are at the edge of structural stability. More exact numbers for the activation energies could be obtained if compounds were to become available that fulfil three requirements: Stable to 200 °C, intrinsically small line width for the metal-bound fluorine atoms, and nonaggressivity (at least towards quartz), so that Teflon inserts in the NMR tubes are no longer required. If one were out to find a hexafluoride that is even less rigid, then $TcF_6^+$ would be the best choice. However, attempts to isolate this compound have so far been unsuccessful.[14]

## Experimental Section

**General**: All reactions were carried out under a dry argon atmosphere (for example, by handling in a dry box with $H_2O$ and $O_2$ content lower than 1 ppm). Solvents were dried by standard methods. Commercially available chemicals ($MoF_6$, $WF_6$, $C_6F_5OH$, $(CH_3)_3SiCl$, $(CF_3)_3COH$, and *n*BuLi) were used as received. The 2,2,2-trifluoroethanol was distilled twice before use. NMR spectra were recorded by using a JEOL JNM-LA 400 spectrometer ($^1$H at 399.65 MHz, $^{13}$C at 100.40 MHz, and $^{19}$F at

Table 5. Rate constants *k* [s$^{-1}$] at different temperatures [K] for $CF_3{-}CH_2{-}O{-}MF_5$, $C_6F_5{-}O{-}MF_5$, M = W, Mo, and $(CF_3)_3C{-}O{-}WF_5$ obtained by simulations using the 3+3 exchange mode.

| $CF_3{-}CH_2{-}O{-}WF_5$ | | $C_6F_5{-}O{-}WF_5$ | | $(CF_3)_3C{-}O{-}WF_5$ | | $CF_3{-}CH_2{-}O{-}MoF_5$ | | $C_6F_5{-}O{-}MoF_5$ | |
|---|---|---|---|---|---|---|---|---|---|
| 5.3 | 313 | 5.1 | 303 | 0.10 | 293 | 303 | 35.6 | 273 | 135.1 |
| 9.4 | 323 | 20.5 | 324 | 0.29 | 303 | 313 | 71.6 | 278 | 196.9 |
| 16.8 | 333 | 80.5 | 344 | 0.71 | 313 | 323 | 138.0 | 283 | 299.2 |
| 33.2 | 343 | 250.0 | 363 | 3.80 | 333 | 333 | 256.0 | 288 | 444.0 |
| 58.9 | 353 | 645.0 | 383 | 14.26 | 353 | 343 | 460.1 | 293 | 656.4 |
| 170.1 | 373 | 1615.0 | 403 | 27.57 | 363 | 353 | 796.1 | 298 | 926.6 |
| 440.8 | 393 | | | 45.62 | 373 | 363 | 1340.2 | 303 | 1332.0 |
| | | | | | | | | 313 | 2702.7 |
| | | | | | | | | 323 | 5405.4 |
| | | | | | | | | 333 | 9459.5 |

  

376.00 MHz). NMR spectra for $C_6F_5$–O–$WF_5$ at 20 °C and 184 °C were recorded by using a JEOL F 90 Q instrument ($^{19}$F at 84.25 MHz). Chemical shift values are reported with respect to TMS ($^1$H, $^{13}$C) and $CCl_3F$ ($^{19}$F). Deuterated solvents were used as received. NMR spectra were recorded at room temperature unless otherwise stated. The $^{19}$F NMR dynamic spectra were measured by using $C_2D_2Cl_4$ as solvent, occasionally $CD_2Cl_2$ was used. Raman spectra were recorded on a Bruker RFS 100 FT-Raman spectrometer. Elemental analyses were performed by Beller Co., Göttingen, Germany.

Single crystals were handled in a special device, cut to an appropriate size, and mounted on a Bruker SMART CCD 1000 TU diffractometer, using $Mo_{K\alpha}$ irradiation, a graphite monochromator, a scan width of 0.3° in $\omega$, and a measurement time of 20 *s* per frame. After semiempirical absorption corrections (SADABS) by equalizing symmetry-equivalent reflections, the SHELX programs were used for solution and refinement.[15] All atoms except hydrogen were refined anisotropically. Hydrogen atoms were located by difference Fourier maps and refined independently from other atomic positions but with a single isotropic displacement parameter for all hydrogen atoms. Experimental details are laid down in Table 6, results in Table 4, see also Figure 2. CCDC-218240 ($C_6F_5$–O–$MoF_5$) and CCDC-218241 ($(CF_3CH_2O)_2MoF_4$) contain the supplementary crystallographic data for this paper. These data can be obtained free of charge via www.ccdc.can.ac.uk/conts/retrieving.html (or from the Cambridge Crystallographic Center, 12 Union Road, Cambridge CB21EZ, UK; Fax: (+44) 1223-336033; or deposit@ccdc.cam.ac.uk).

Table 6. Crystallographic data.

| Compounds | $C_6F_5$–O–$MoF_5$ | *cis*-$[(CF_3CH_2O)_2MoF_4]$ |
|---|---|---|
| $M$ | 374.00 | 370.01 |
| $T$ [°C] | −100 | −100 |
| space group | $P2_1/n$ | $P\bar{1}$ |
| $a$ [pm] | 647.6(1) | 1008.6(1) |
| $b$ [pm] | 1256.7(3) | 1041.3(1) |
| $c$ [pm] | 1123.1(2) | 1085.9(1) |
| α [°] | 90 | 73.499(2) |
| β [°] | 91.400(4) | 74.614(2) |
| γ [°] | 90 | 89.603(2) |
| $V$ [$10^6$ pm$^3$] | 913.8 | 1051.5 |
| $Z$ | 4 | 4 |
| μ [mm$^{-1}$] | 1.58 | 1.38 |
| $\theta_{max}$ [°] | 30.6 | 30.6 |
| reflections collected | 11435 | 13084 |
| reflections, independent | 2802 | 6340 |
| refined parameters | 163 | 308 |
| $R$ | 0.029 | 0.068 |
| $wR_2$ | 0.068 | 0.206 |

The program *g*NMR was used for the simulation of the dynamic NMR spectra.[16] DFT calculations were performed with the program GAUSSIAN revision A7, 1998,[17] method Becke 3 LYP, as implemented in the program. Basis sets: 6–311G(d,p) for C, H, O, and F. The relativistically corrected pseudopotentials and basis sets for Cr, Mo, W, Nb, Tc, and Re were obtained from the Institut für Theoretische Chemie, Universität Stuttgart. Cr: 10 core electrons; Nb, Mo, Tc: 28 core electrons; W, Re: 60 core electrons, 8s 7p 6d valency basis for each metal.

**(2,2,2-Trifluoroethoxy)trimethylsilane ($CF_3$–$CH_2$–O–$Si(CH_3)_3$)**: (2,2,2-Trifluoroethoxy)trimethylsilane was prepared by using a literature procedure.[18] Bis(trimethylsilyl)amine (45 mL, 0.212 mol) and two drops of chlorotrimethylsilane were added under argon pressure to a previously dried three-neck flask equipped with a reflux condenser. With the aid of a syringe, 2,2,2-trifluoroethanol (30 mL, 0.417 mol) was added dropwise while the mixture was stirred slowly. After the mixture had been refluxed for three hours, the liquid was distilled at atmospheric pressure to give a mixture of $CF_3$–$CH_2$–O–$Si(CH_3)_2$ and $[(CH_3)_3Si]_2NH$ (84% and 16%, respectively, as shown by the $^1$H NMR integrals). The mixture was evacuated at −30 °C and with the aid of a double cold trap (−60 °C/−196 °C) $CF_3$–$CH_2$–O–$Si(CH_3)_3$ (59.58 g; 83% yield) was collected as a colorless liquid in the −196 °C trap. $^1$H NMR ($CDCl_3$): $\delta$ = 3.9 (q, $^3J_{F,H}$ = 8.66 Hz, 2H; $-CH_2-$), 0.1 ppm (s, 9H; $-CH_3$); $^{13}$C{$^1$H} NMR ($CDCl_3$): $\delta$ = 124.3 (q, $^1J_{C,F}$ = 278.6 Hz, 1C; $-CF_3$), 61.2 (q, $^2J_{C,F}$ = 35.7 Hz, 1C; $-CH_2-$), −0.9 ppm (s, 3C; $-CH_3$); $^{19}$F NMR ($CDCl_3$): $\delta$ = −77.4 ppm (t, $^3J_{F,H}$ = 7.7 Hz, 3F; $-CF_3$).

**(Pentafluorophenoxy)trimethylsilane ($C_6F_5$–O–$Si(CH_3)_3$)**: (Pentafluorophenoxy)trimethylsilane was prepared in a similar manner to the procedure described above, as the reaction between pentafluorophenol and chlorotrimethylsilane reported in the literature proved to be unreliable.[19] Pentafluorophenol (30.0 g, 0.163 mol) was added to a previously dried three-neck flask equipped with a reflux condenser. $[(CH_3)_3Si]_2NH$ (18 mL, 84.7 mmol) was added dropwise slowly into the flask followed by stirring as soon as there was enough liquid. The reaction mixture was refluxed for 4 h. After distillation, the mixture contained 85% $C_6F_5$–O–$Si(CH_3)_3$ and 15% bis(trimethylsilyl)amine. Vacuum distillation from −30 °C into a −196 °C trap gave the pure compound (25.05 g; 60% yield) as a colorless liquid. $^1$H NMR ($CDCl_3$): $\delta$ = 0.1 ppm (s, 9H; $-CH_3$); $^{13}$C{$^{19}$F} NMR ($CDCl_3$): $\delta$ = 138.6 (s, 1C; $C_{2,6}$), 135.640 (s, 1C; $-C_{3,5}$), 133.7 (s, 1C; $-C_4$), 128.1 (s, 1C; $-C_1$), −1.6 ppm (q, $^1J_{C,H}$ = 119.5 Hz, 3C; $-CH_3$); $^{19}$F NMR ($CDCl_3$): $\delta$ = −159.7 (d, $^3J_{F,F}$ = 18.4 Hz, 2F; *-o*), −165.8 (t, $^3J_{F,F}$ = 21.3 Hz, 2F; *-m*), −168.2 ppm (t, $^3J_{F,F}$ = 21.3 Hz, 1F; *-p*).

**Lithium perfluoro(*tert*-butoxide) ($LiOC(CF_3)_3$)**: Lithium perfluoro(*tert*-butoxide) was prepared in a similar manner to a literature procedure.[20] Perfluoro(*tert*-butyl aclohol) (1.5 mL, 10.74 mmol) was added under argon pressure to a previously dried three-neck flask equipped with a reflux condenser. With the aid of a syringe, *n*BuLi (1.6 M in hexane, 6.7 mL, 10.72 mmol) was added dropwise while the mixture was stirred at room temperature. After the reaction mixture was refluxed for 4 h, the flask was cooled down and kept at 0 °C while all volatile materials were pumped off over a period of 6 h. A yellowish oily material remained in the flask. After the material was sublimed (48 h/150 °C/$10^{-3}$ mbar), a white crystalline material identified as $LiOC(CF_3)_3$ (0.51 g; 19.6% yield) was recovered. $^{13}$C{$^{19}$F} NMR ($Et_2O/CDCl_3$): $\delta$ = 122.1 (s, 3C; $-CF_3$), 81.1 ppm (s, 1C; −OC); $^{19}$F NMR ($Et_2O/CDCl_3$): $\delta$ = −77.3 ppm (s, 9F; $-CF_3$).

**Tungsten pentafluoride (2,2,2-trifluoroethoxide) ($CF_3$–$CH_2$–O–$WF_5$)**: A mixture of $CF_3$–$CH_2$–O–$Si(CH_3)_3$ (1.590 g, 9.23 mmol) with a few drops of 2,2,2-trifluoroethanol was added to a previously dried PFA tube equipped with a magnetic stirrer. An excess of $WF_6$ (7.41 g, 24.91 mmol) was condensed into this mixture. The reaction vessel was kept at −90 °C over a period of 3 h. The temperature was allowed to rise up to −30 °C while the mixture was being stirred. At this point a light pink solution was observed. The mixture was kept at −30 °C and stirred for a further 1 h. The PFA tube was kept between −40 °C and −30 °C while it was evacuated for 5 h, a transparent liquid (3.313 g; 95% yield), highly sensitive to moisture and slightly volatile at room temperature, remained inside the tube. M.p. −55.5 °C; $^{13}$C{$^1$H} NMR ($CDCl_3$ ext.): $\delta$ = 121.4 (q, $^1J_{C,F}$ = 278.9 Hz, 1C; $-CF_3$), 76.7 ppm (q, $^2J_{C,F}$ = 40.2 Hz, 1C; $-CH_2-$); $^{19}$F NMR ($CDCl_3$ ext.): $\delta$ = 129.2 (d, $^2J_{F,F}$ = 64.0 Hz, 4F; $F_{eq.}$), 107.5 (q, $^2J_{F,F}$ = 66.3 Hz, 1F; $F_{ax.}$), −75.6 ppm (s, 3F; $-CF_3$); Raman spectroscopy: $\tilde{\nu}$ = 3022(4), 2971(14), 2864(1), 2772(1), 1437(12), 1395(5), 1279(15), 1145(38), 950(7), 841(41), 732(100), 638(16), 618(41), 528(29), 360(28), 306(59), 247(12), 187(9), 123(33) cm$^{-1}$; elemental analysis calcd (%): C 6.36, H 0.53; found: C 6.93, H 0.65.

**Molybdenum pentafluoride (2,2,2-trifluoroethoxide) ($CF_3$–$CH_2$–O–$MoF_5$)**: In a dry box, a mixture of $CF_3$–$CH_2$–O–$SiR_3$ (0.901 g, 5.23 mmol) with a few drops of 2,2,2-trifluoroethanol was placed in a previously dried PFA tube equipped with a magnetic stirrer. An excess of $MoF_6$ (2.779 g, 13.24 mmol) was condensed into this mixture. At −78 °C, various colors (yellow, light brown, light green) were observed at the contact surface between the two reactants. The mixture was maintained and stirred at −50 °C for 2 h. The PFA tube with the dark brown mixture was evacuated between −75 °C and −60 °C for 3 h. Three more hours at −30 °C of evacuation were needed to pump off all unreacted $MoF_6$. A light yellow liquid (1.432 g; 94.4% yield), very reactive to moisture and slightly volatile at room temperature, remained inside the tube. M.p. −31.0 °C; $^{13}$C{$^1$H} NMR ($CDCl_3$ ext.): $\delta$ = 122.9 (q, $^1J_{C,F}$ = 280.13 Hz, 1C; $-CF_3$), 84.8 ppm (q, $^2J_{C,F}$ = 39.98 Hz, 1C; $-CH_2-$); $^{19}$F NMR ($CDCl_3$ ext.): $\delta$ = 234.8 (d, $^2J_{F,F}$ = 82.4 Hz, 4F; $F_{eq.}$), 207.5 (q, $^2J_{F,F}$ = 87.7 Hz, 1F; $F_{ax}$), −71.1 ppm (s, 3F; $-CF_3$); Raman spectroscopy: $\tilde{\nu}$ = 30.10(6), 2953(21), 2838(1), 2747(1), 1424(14), 1382(14), 1267(19), 1098(82),

944(8), 840(44), 701(100), 641(41), 608(65), 530(45), 383(41), 357(22), 324(66), 302(56), 246(21), 172(18), 122(56) $cm^{-1}$; elemental analysis calcd (%): C 8.28, H 0.69; found: C 8.73, H 0.76.

**Molybdenum bis (2,2,2 trifluoroethoxide) tetrafluoride (*cis*-[$(CF_3CH_2O)_2MoF_4$])**: In an attempt to synthesize $CF_3–CH_2–O–MoF_5$ as described in the literature,[21,22] a mixture of compounds with the molecular formula $(CF_3–CH_2–O)_nMF_{6-n}$, $n$ = 1, 2, and 3 (as shown by the $^{19}F$ NMR spectroscopy) was obtained. After letting the sample stand for a few days at room temperature, some yellow crystals were observed on the walls of the reaction flask. The crystals were suitable for X-ray diffraction (see Table 6). The structure obtained was *cis*-[$(CF_3–CH_2–O–)_2MoF_4$]. Attempts to crystallize the *trans* derivative or the other higher members of the series from this mixture failed, and no other substance could be isolated. $^{19}F$ NMR {$CDCl_3$ ext): $\delta$ = 171.3 (t, $^2J_{F,F}$ = 91.5 Hz, 2F), 151.9 (t, $^2J_{F,F}$ = 91.5 Hz, 2F), −74.6 ppm (s, 3F).

**Tungsten pentafluoride pentafluorophenoxide ($C_6F_5–O–WF_5$)**: Attempts to synthesize a pure sample according to reported procedures[23,24] were all unsuccessful. Even modifications on the procedure, such as the use of a solvent ($CH_2Cl_2$, $CCl_3F$), higher reaction temperatures, and longer reaction times, gave either unreacted $WF_6$ and $C_6F_5–O–Si(CH_3)_3$ or a mixture of compounds with the molecular formula $(C_6F_5O)_nWF_{6-n}$, $n$ = 1, 2, 3 as shown by the $^{19}F$ NMR spectra. No possible purification of the desired compound was achieved.

A solution of $C_6F_5–O–Si(CH_3)_3$ (3.610 g, 14.09 mmol) and $C_6F_5OH$ (0.099 g, 0.54 mmol) was placed in a previously dried PFA tube equipped with a stainless steel valve. An excess of $WF_6$ (12.119 g, 40.69 mmol) was condensed into the tube. The reaction mixture was stirred at −5 °C for seven days. The reaction vessel was evacuated at −45 °C for 4 h. Two more hours of evacuation at −30 °C were needed to pump off all unreacted $WF_6$. A red-orange solid (6.44 g) remained inside the tube. $CCl_3F$ at −30 °C was added to the reaction vessel with a Teflon tube; most of the material was insoluble at this temperature, but at −15 °C almost everything dissolved. By means of a Teflon tube, the solution was transferred at −15 °C to a new PFA tube; $^{19}F$ and $^{13}C$ NMR spectra of the sample were obtained at the same temperature, and revealed signals for only one kind of $C_6F_5–O–$ compound. The PFA tube was evacuated at −15 °C for 6 h. A red solid material (6.081 g; 89.9 % yield), extremely reactive towards moisture, remained in the tube. M.p. −1.5 °C; $^{13}C\{^{19}F\}$ NMR ($CDCl_3$ ext.): $\delta$ = 143.2 (s, 1C; $-C_4$), 142.4 (s, 2C; $-C_{2,6}$), 137.0 (s, 2C; $-C_{3,5}$), 134.2 ppm (s, 1C; $-C_1$); $^{19}F$ NMR (376 MHz, 20 °C, $CDCl_3$ ext.): $\delta$ = 144.3 (d, $^2J_{F,F}$ = 64.3, $^1J_{W,F}$ = 40 Hz, 4F; $F_{eq.}$), 136.6 (q, $^2J_{F,F}$ = 65.6 Hz, 1F; $F_{ax.}$), −150.6 (t, $^3J_{F,F}$ = 18.5 Hz, 1F; $-p$), −151.7 (d, $^3J_{F,F}$ = 12 Hz, 2F; $-o$), −160.7 ppm (t, $^3J_{F,F}$ = 17.0 Hz, 2F; $-m$); $^{19}F$ NMR (84.25 MHz, 184 °C, 1.04 M, $CCl_2DCCl_2D$): $\delta$ = 145.7 ppm (s, $^1J_{W,F}$ = 40 Hz, 5F); Raman spectroscopy: $\tilde{\nu}$ = 1641(15), 1535(3), 1517(3), 1466(100), 1325(33), 1263(3), 118(31), 1160(4), 1051(18), 1041(22), 1018(5), 787(6), 765(33), 720(18), 714(27), 653(4), 641(6), 583(5), 501(15), 452(7), 423(13), 406(6), 377(9), 336(10), 307(9), 297(8), 280(20), 262(12), 224(6), 201(6), 185(6), 155(11), 120(8) $cm^{-1}$; elemental analysis calcd (%): C 15.60; found: C 16.46.

**Molybdenum pentafluoride pentafluorophenoxide ($C_6F_5–O–MoF_5$)**: $MoF_6$ (1.830 g, 8.72 mmol) and $CH_2Cl_2$ (1.160 g, 13.82 mmol) were condensed into a previously dried PFA tube equipped with a magnetic stirrer. A solution of $C_6F_5–O–Si(CH_3)_3$ (1.311 g, 5.12 mmol) and $C_6F_5OH$ (0.069 g, 0.37 mmol) was added dropwise with a syringe, while the reaction mixture was stirred and kept at −20 °C. Additional $CH_2Cl_2$ (1.32 g, 15.73 mmol) was added to wash down the inner walls of the tube. After the dark purple solution was stirred for 2 weeks at −20 °C, a black precipitate was observed. The PFA tube was evacuated first at −50 °C for 1 h and then at −20 °C for 5 h. A black solid crystalline material 1.69 g, 82.5 % yield), extremely reactive to moisture, remained in the tube. Crystals suitable for X-ray diffraction were taken from this sample (Table 6). M.p. 57.3–58 °C; $^{13}C\{^{19}F\}$ NMR (−20 °C, 0.35 M, $Cl_2CDCDCl_2$): $\delta$ = 147.2 (s, 1C; $-C_4$), 145.2 (s, 2C; $-C_{2,6}$), 136.8 ppm (s, 2C; $-C_{3,5}$); $^{19}F$ NMR (−20 °C, 0.35 M, $Cl_2CDCDCl_2$): $\delta$ = 254.5 (d, $^2J_{F,F}$ = 82.0 Hz, 4F; $F_{eq.}$), 250.2 (q, $^2J_{F,F}$ = 88.5 Hz, 1F; $F_{ax.}$), −134.9 (t, $^3J_{F,F}$ = 20.0 Hz, 1F; $-p$), −140.8 (d, $^3J_{F,F}$ = 15 Hz, 2F; $-o$), −154.9 (t, $^3J_{F,F}$ = 18.5 Hz, 2F; $-m$); Raman spectroscopy: $\tilde{\nu}$ = 1636(25), 1507(6), 1424(45), 1397(49), 1380(15), 1320(77), 1183(57), 1039(75), 1017(21), 789(9), 732(100), 697(45), 669(60), 640(12), 622(10), 604(23), 580(40), 496(84), 447(12), 405(11), 384(23), 366(25), 353(20), 306(53), 290(48), 252(13), 226(14), 208(15), 196(16), 178(17), 156(12), 111(16) $cm^{-1}$; elemental analysis calcd (%): C 19.27; found: C 18.34.

**Tungsten pentafluoride (*tert*(perfluoro)butoxide) ($(CF_3)_3C–O–WF_5$)**: $LiOC(CF_3)_3$ (0.326 g, 1.496 mmol) was added to a previously dried PFA tube equipped with a magnetic stirrer. An excess of $WF_6$ (1.83 g, 6.144 mmol) was condensed into the tube. After the reaction mixture had been stirred at room temperature for 4.5 days, an $^{19}F$ NMR spectrum of the solution showed $F_5W–O–C(CF_3)_3$ as the only main product. The PFA tube was cooled to −50 °C and warmed up gradually to 0 °C over a period of 18 h, while all volatile materials were pumped off into two traps (−78 °C/−196 °C). A colorless liquid (0.47 g, 61.1 % yield) identified as $F_5W–O–C(CF_3)_3$ was recovered in the −78 °C trap. M.p. −59 °C; $^{13}C\{^{19}F\}$ (0 °C, $Cl_2CDCDCl_2$): $\delta$ = 118.2 (s, 3C; $-CF_3$), 85.8 (s, 1C; $-OC$); $^{19}F$ NMR (0 °C, $Cl_2CDCDCl_2$): $\delta$ = 150.0 (d, $^2J_{F,F}$ = 64.8 Hz, 4F; $F_{eq.}$), 157.5 (q, $^2J_{F,F}$ = 65.18 Hz, 1F; $F_{ax}$), −74.8 ppm (s, 9F; $-CF_3$). Raman specrtroscopy: $\tilde{\nu}$ = 1316(10), 1273(10), 1229(5), 1177(23), 986(2), 859(12), 761(88), 735(100), 674(10), 659(14), 539(16), 426(4), 333(49), 305(67), 284(55), 241(19), 134(39), 113(24) $cm^{-1}$.

**$^{19}F$ NMR input parameters for the simulations in *g*NMR: $CF_3–CH_2–O–WF_5$**: Sample concentration: 1.52 M (in $C_2D_2Cl_4$); $^2J_{Fax,Feq}$ = 65.80 Hz, $^1J_{W,Fa}$ = 44.20 Hz, $^1J_{W,Feq}$ = 39.57 Hz; line width (Hz; A part, $B_4$ part) : 14, 16; temperature (K)/chemical shift (ppm; A part, $B_4$ part): 313/108.982, 129.777; 323/109.671, 130.12; 333/111.226, 131.123; 343/111.900, 131.365; 353/112.458, 131.438; 373/113.770, 131.928; 393/115.275, 470.

**$C_6F_5–O–WF_5$**: Sample concentration: 1.035 M (in $C_2D_2Cl_4$); $^2J_{Fax,Feq}$ = 66.00 Hz, $^1J_{W,Fa}$ = 61.20 Hz, $^1J_{W,Feq}$ = 35.90 Hz; line width (Hz; A part, $B_4$ part): 15, 12; temperature (K)/chemical shift (ppm; A part, $B_4$ part): 303/143.948, 147.229; 324/144.925, 147.588; 344/145.755, 147.926; 363/146.380, 148.222; 383/147.135, 148.535; 403/147.939, 148.794.

**$(CF_3)_3C–O–WF_5$**: Sample concentration: 0.526 M (in $C_2D_2Cl_4$); $^2J_{Fax,Feq}$ = 65.30 Hz, $^1J_{W,Fa}$ = 65.18 Hz, $^1J_{W,Feq}$ = 34.90 Hz; line width (Hz; A part, $B_4$ part): 3.6, 6.2; temperature (K)/chemical shift (ppm; A part, $B_4$ part): 293/158.073, 150.332; 303/158.327, 150.441; 313/158.576, 150.552; 333/159.059, 150.778; 353/159.528, 151.014; 363/159.750, 151.130; 373/159.946, 151.252.

**$CF_3–CH_2–O–MoF_5$**: Sample concentration 1.249 M (in $C_2D_2Cl_4$); $^2J_{Fax,Feq}$ = 89.68 Hz; line width (Hz; A part, $B_4$ part): 38, 30. Temperature (K)/chemical shift (ppm; A part, $B_4$ part): 303/215.947, 233.646; 313/217.053, 233.934; 323/218.110, 234.200; 333/219.200, 234.472; 343/220.150, 234.750; 353/221.100, 235.030; 363/222.800, 235.280.

**$C_6F_5–O–MoF_5$**: Sample concentration 0.259 M (in $C_2D_2Cl_4$); $^2J_{Fax,Feq}$ = 91.50 Hz; line width (Hz; A part, $B_4$ part): 25, 29; temperature (K)/chemical shift (ppm; A part, $B_4$ part): 273/243.251, 249.189; 278/243.774, 249.295; 283/244.290, 249.405; 288/244.802, 249.518; 293/245.305, 249.629; 298/245.804, 249.741; 303/246.290, 249.858; 313/247.232, 250.090; 323/248.328, 250.328; 333/249.187, 250.558.

## Acknowledgement

The authors are indebted to the Deutsche Forschungsgemeinschaft and the Fonds der Chemischen Industrie for financial support. Thanks are also due to Dr. P. Budzelaar for some introduction into *g*NMR.

[1] For reviews on this subject see: K. Seppelt, *Acc. Chem. Res.* **2003**, *36*, 147–153; M. Kaupp, *Angew. Chem.* **2001**, *113*, 3642–3677; *Angew. Chem. Int. Ed.* **2001**, *40*, 3534–3565.
[2] G. A. Seisenbaeva, L. Kloo, P. Werndrup, V. G. Kessler, *Inorg. Chem.* **2001**, *40*, 3815–3818.
[3] A. Haaland, K. Rypdal, H. Volden, E. Jacob, J. Weidlein, *Acta Chem. Scand.* **1989**, *43*, 911–913.
[4] D. C. Bradley, M. H. Chisholen, C. E. Heath, M. B. Hursthouse, *J. Chem. Soc. Chem. Commun.* **1969**, 1261.
[5] H. M. Seip, R. Seip, *Acta Chem. Scand.* **1966**, *20*, 2698–2710.
[6] H. H. Claassen, G. L. Goodman, J. H. Holloway, H. Selig, *J. Chem. Phys.* **1970**, *53*, 347–348.
[7] R. T. Paine, R. S. McDowell, L. B. Asprey, L. H. Jones, *J. Chem. Phys.* **1976**, *64*, 3081–3083.

  

[8] M. Kimura, V. Schonakev, D. W. Smith, B. Weinstock, *J. Chem. Phys.* **1968**, *48*, 4001–4012.
[9] A. D. Richardson, K. Hedberg, G. M. Lucier, *Inorg. Chem.* **2000**, *39*, 2787–2793.
[10] R. Marx, K. Seppelt, R. M. Ibberson, *J. Chem. Phys.* **1996**, *104*, 7658–7664.
[11] R. Wesendrup, P. Schwerdtfeger, *Inorg. Chem.* **2001**, *40*, 3351–3354.
[12] J. C. Bailar, Jr., *J. Inorg. Nucl. Chem.* **1958**, *8*, 165.
[13] For $\beta = 90°$ a bicapped tetrahedral structure is obtained, as discussed by: R. Hoffmann, J. M. Howell, A. R. Rossi, *J. Am. Chem. Soc.* **1976**, *98*, 2484–2492.
[14] N. Le. Blond, H. P. A. Mercier, D. A. Dixon, G. J. Schrobilgen, *Inorg. Chem.* **2000**, *39*, 4494.
[15] G. Sheldrick, Program for Crystal Structure Solution; University of Göttingen, Germany, **1986**. G. Sheldrick, SHELXS-93, University of Göttingen, Germany, **1993**.
[16] *g*NMR, version 5.0.1.0, P. H. M. Budzelaar **2002**, Adept Scientific plc, U.K.
[17] Gaussian 98 (Revision A.7), M. J. Frisch, G. W. Trucks, H. B. Schlegel, G. E. Scuseria, M. A. Robb, J. R. Cheeseman, V. G. Zakrzewski, J. A. Montgomery, Jr., R. E. Stratmann, J. C. Burant, S. Dapprich, J. M. Millam, A. D. Daniels, K. N. Kudin, M. C. Strain, O. Farkas, J. Tomasi, V. Barone, M. Cossi, R. Cammi, B. Mennucci, C. Pomelli, C. Adamo, S. Clifford, J. Ochterski, G. A. Petersson, P. Y. Ayala, Q. Cui, K. Morokuma, D. K. Malick, A. D. Rabuck, K. Raghavachari, J. B. Foresman, J. Cioslowski, J. V. Ortiz, B. B. Stefanov, G. Liu, A. Liashenko, P. Piskorz, I. Komaromi, R. Gomperts, R. L. Martin, D. J. Fox, T. Keith, M. A. Al-Laham, C. Y. Peng, A. Nanayakkara, C. Gonzalez, M. Challacombe, P. M. W. Gill, B. G. Johnson, W. Chen, M. W. Wong, J. L. Andres, M. Head-Gordon, E. S. Replogle, J. A. Pople, Gaussian, Inc., Pittsburgh, PA, **1998**
[18] S.H. Langer, S. Connell, I. Wender, *J. Org. Chem*, **1958**, 23, 50–58.
[19] A. J. Oliver, W. A. Graham, *J. Organomet. Chem.* **1969**, *19*, 17–26.
[20] R. E. Dear, W. B. Fox, R. J. Fredericke, E. E. Gilbert, D. K. Huggins, *Inorg. Chem.* **1970**, *9*, 2590–2591.
[21] F. E. Brinckman, R. B. Johannesen, R. F. Hammerschmidt, L. B. Handy, *J. Fluorine Chem.* **1975**, *6*, 427–436.
[22] L. B. Handy, *J. Fluorine Chem.* **1976**, *7*, 641–645.
[23] F. E. Brinckman, R. B. Johannesen, L. B. Handy, *J. Fluorine Chem.* **1971**, *1*, 493–497.
[24] A. Majid, D. W. A. Sharp, J. M. Winfield, I. Hanley, *J. C. S. Dalton Trans.* **1973**, 1876–1878.

Received: January 30, 2004
Published online: August 13, 2004

  